Groundwater
Monitoring&Remediation

Reliable Monitoring of the Transition Zone Between Fresh and Saline Waters in Coastal Aquifers

by Elad Levanon, Yoseph Yechieli, Eyal Shalev, Vladimir Friedman, and Haim Gvirtzman

Abstract

This study deals with the reliability of monitoring the transition zone between fresh and saline waters in coastal aquifers, considering the effect of tides in long-perforated boreholes. Electric conductivity (EC) fluctuations in the coastal aquifer of Israel, as measured in long-perforated borehole, were found to have the same periodicities as the sea tide, though some orders of magnitude larger than sea-level or groundwater level fluctuations. Direct measurements in the aquifer through buried EC sensors demonstrate that EC measurements within the long-perforated boreholes might be distorted due to vertical flow in the boreholes, whereas actual fluctuations of the transition zone within the aquifer are some orders of magnitude smaller. Considering these field data, we suggest that monitoring of the transition zone between fresh and saline water adjacent to the sea through long-perforated boreholes is unreliable. EC fluctuations in short-perforated boreholes (1 m perforation at the upper part of the transition zone) were somewhat larger than in the aquifer, but much smaller than those in the long-perforated borehole. The short-perforation diminishes the vertical flow and the distortion and therefore is more reliable for monitoring the transition zone in the shoreline vicinity.

Introduction

The transition zone between the fresh groundwater and the saline sea water, which occurs in coastal aquifers, is a well-known phenomenon that has been extensively studied in the past. Many studies have dealt with the development of the transition zone and the regional flow regimes (Cooper 1959; Kohout 1960; Bear 1979; Todd 1980) and with processes affecting the depth, the thickness and other changes of the transition zone due to natural and anthropogenic causes (Bear 1972; Strack 1976; Ataie-Ashtiani et al. 1999; Van Dam 1999; Wang and Tsay 2001).

In coastal aquifers with relatively high permeability, tidal fluctuations induce groundwater level fluctuations with periodicity similar to tide periodicity (Nielsen 1990). As a tidal wave propagates inland through an aquifer, the amplitude of groundwater head fluctuations is progressively decreased. It was claimed that sea tide causing groundwater fluctuations is the main process resulting in the mixing between the fresh and saline waters (Underwood et al. 1992). Monitoring of temporal fluctuations in the transition zone adjacent to the shoreline in an unconfined aquifer in Sydney, Australia, did not show significant fluctuations in response to tide (Cartwright et al. 2004). Nor did electric conductivity (EC) profiles which were taken in an unconfined coastal aquifer in Jeju Island, Korea, in boreholes located 0.9 to 1.7 km from the shoreline at different stages of the tide show significant fluctuations (Kim et al. 2006).

Since the late 1980s, the use of long-perforated boreholes for groundwater sampling and monitoring was countered by many studies. Vertical flow can occur in the borehole due to a vertical hydraulic gradient (Church and Granato 1996). The borehole, which has a much higher hydraulic conductivity compared to the aquifer, acts as a "short circuit" between the higher and lower hydraulic head zones (Elci et al. 2001). Using an analytical model, Robbins (1989) showed that sampling from long-perforated boreholes might be biased because of dilution by flow within the borehole. Comparison between water samples from long- and short-perforated boreholes in an unconfined sandy aquifer demonstrates that the samples from the long-perforated borehole did not represent the aquifer accurately (Church and Granato 1996). Konikow and Hornberger (2006) used a three-dimensional flow and transport model to show that long-perforated boreholes form preferential pathways for groundwater.

Although there are several studies that deal with the long-perforation effect on groundwater, they usually do not deal with the effect of long-perforated boreholes on monitoring the transition zone between fresh and saline water in observation boreholes.

Kim et al. (2005) monitored the groundwater level and EC in a borehole 60 m from the shoreline in a confined coastal aquifer in Kimje, Korea. They showed that the groundwater level and EC fluctuations in the transition zone

doi: 10.1111/gwmr.12020

(which were in the range of 7 to 12 mS/cm) were composed of a wave with a periodicity of 15.4 d and a wave with a periodicity of 0.52 d, which is quite similar to the periodicity between neap and spring tides (14.75 d) and the periodicity between the highest or lowest tidal level in a day (0.52 d). Notably, however, these observation wells were completely perforated and may have caused some measurement artifacts.

In a long-perforated observation borehole in the coastal aquifer of Israel, Shalev et al. (2009) showed significant fluctuations of EC in the transition zone with a periodicity similar to that of the tide. However, the amplitude of the EC fluctuations was an order of magnitude larger than that of the sea tide or the groundwater level. The fluctuation of the transition zone in the borehole was found to be on the order of 2 to 3 m. They showed by a 3D numerical model that vertical flow, which occurs in the borehole due to the long-perforation and does not occur in the aquifer itself, causes that bias.

The objective of this study was to develop and exhibit a more reliable method for monitoring the location of the transition zone and to compare it to previous methods. In all previous field studies of the transition zone, measurements were made within boreholes. In this research, for the first time, in addition to measurements in boreholes, the location of the transition zone was measured directly in the aquifer itself.

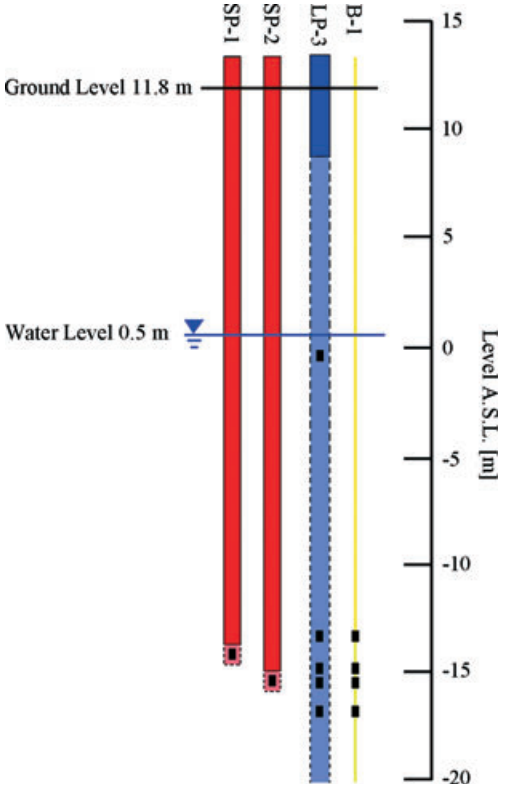

Figure 2. Location of sensors in LP-3, SP-1, SP-2 and B-1, all located 70 m from shoreline. The broken line represents the perforated segment of the borehole. Note that borehole LP-3 is deeper than shown in this figure.

Research Area

This research was conducted in the Israeli coastal aquifer adjacent to the Mediterranean Sea. The length of the aquifer is 120 km, and its width varies from 8 km in the north to about 30 km in the south (Figure 1). The Kurkar Group, which forms the aquifer, is composed mostly of sand, calcareous sandstone ("Kurkar"), siltstone and marine clay and shale of Pleistocene age (Issar 1968; Nativ and Weisbrod 1994). These clay lenses divide the aquifer into several sub-aquifers, mainly at the western part of the aquifer. In this research, we deal only with the upper, unconfined sub-aquifer. The coastal aquifer lies above the Saqiye Group, which is an impermeable clay of Neogene age. The general flow direction in the aquifer is from east to west, toward the Mediterranean Sea, and the hydraulic conductivity of the coastal aquifer in the research area was estimated to be

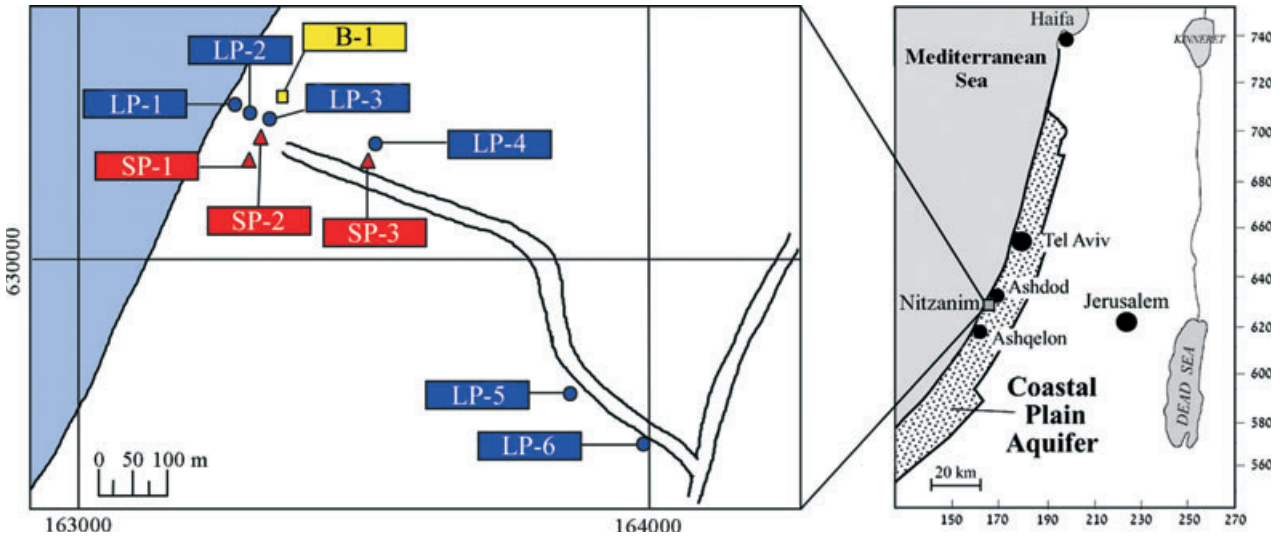

Figure 1. Location map and research area. Blue circles: Long-perforated (LP-X) boreholes, Red triangles: Short-perforated (SP-X) boreholes, Yellow square: location of the buried (B-X) sensors. Coordinates are in ITM grid. The black lines represent a dirt road.

Table 1

Major Tidal Constituents Typical for Mixed Tide (Based on Boon [2004])

Tidal Constituent	Lunar Declinational Diurnal	Luni-Solar Declinational Diurnal	Larger Lunar Elliptic Semidiurnal	Solar Semidiurnal	Lunar Semidiurnal
Symbol	O_1	K_1	N_2	S_2	M_2
Speed (degree/solar hour)	13.943	15.041	28.440	28.984	30.000
Frequency (solar day^{-1})	0.932	0.999	1.892	1.996	1.930
Periodicity (solar day)	1.073	1.001	0.529	0.501	0.518

5 to 10 m/d, using slug tests (Lutzki and Shalev 2010). Sea water intrusion has been observed over a distance of more than 1-km inland in some areas, due to over-exploitation of the aquifer in the past few decades (Melloul 1988; Melloul and Zeitoun 1999).

The research area is part of the Nitzanim Nature Reservation, 1 km south of Ashdod, in the southern part of the coastal aquifer of Israel, where the annual mean precipitation is 500 mm/year. In this work, we focused on the upper phreatic part of the aquifer (the upper 80 m), which is relatively homogenous, composed of sand and calcareous sandstone ("Kurkar") and almost no clay lenses, except for small lenses, mostly in the unsaturated zone (Figure 3). Being part of a nature reservation, this area has been subject to minimum anthropogenic effects such as agriculture and urban construction. A preliminary study of the transition zone in the Nitzanim area was conducted by Yechieli and Hadad (2009), from several boreholes drilled at different distances from the sea, showing the general configuration of the transition zone. The area near the shoreline itself (<200 m from the shoreline) had not been studied before.

The tidal phenomenon in the Mediterranean Sea is mixed tide, which means that there are two cycles of high- and low-tide in a day, when one high-tide (or low-tide) is higher (or lower) than the next one (Pugh 1996). In this kind of tide, there are five major tidal constituents that compose the tidal wave (Boon 2004): (1) lunar declinational diurnal (O_1); (2) luni-solar declinational diurnal (K_1); (3) larger lunar elliptic semidiurnal (N_2); (4) solar semidiurnal (S_2); and (5) lunar semidiurnal (M_2). The speed, frequency, and periodicity of each constituent are assembled in Table 1. The consequence of the phase lag between the tidal constituents is the difference between neap and spring tides. In the Mediterranean Sea, tidal amplitude varies from approximately 0.4 m at spring tide to approximately 0.1 m at neap tide.

Methods

Research Boreholes

Ten boreholes were drilled perpendicular to the shoreline (Figure 1): six long-perforated (LP), three short-perforated (SP) and one drilled in order to allow burying EC sensors in the aquifer (B). Boreholes LP-1 and LP-2 were drilled 20 and 40 m from the shoreline, respectively; LP-3, SP-1, SP-2 and B-1 were drilled adjacent to each other, all 70 m from the shoreline; LP-4 and SP-3 were drilled 230 m from the shoreline; and LP-5 and LP-6 were drilled 715 and 900 m from the shoreline, respectively. Most of the boreholes

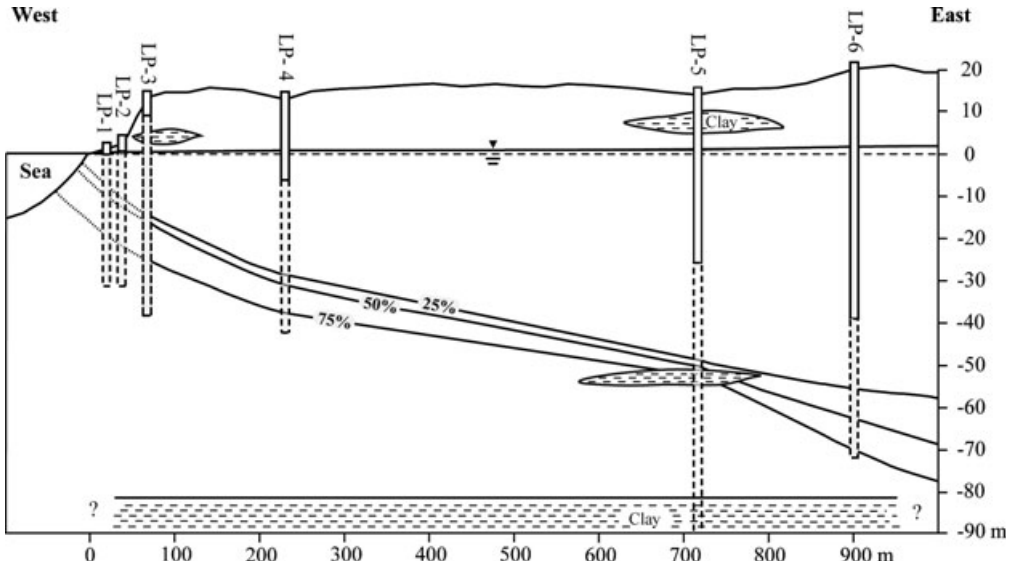

Figure 3. Cross section of the transition zone between fresh and saline waters perpendicular to the shoreline in the research area. Groundwater salinity isopleths are marked by black lines. The broken lines in the boreholes represent the perforated segment. On the vicinity of the shoreline the location of the transition zone was estimated because the groundwater is consistently affected by sea waves.

(except LP-5 and LP-6) were drilled with a dual-system drilling machine with a 2″ drill-bit and 5″ or 6″ casing tubes, using air pressure and without adding drilling mud or water.

All boreholes, except B-1, were outfitted with 2″ diameter PVC tubes and the annular space around the perforations was packed with washed quartz sand. The long-perforated boreholes (LP-1 to 6) are similar to the observation boreholes used for the monitoring of the transition zone along the coastal aquifer, each has perforations in the length of 30 to 100 m. The short-perforated boreholes (SP-1 to 3) have a 1 m perforation at different depths of the transition zone, while the upper part of the PVC tube is sealed.

After completing the drilling of B-1 borehole, the drill-bit was taken out of the borehole and four EC sensors, attached to a 3/4″ PVC pipe, were lowered into the borehole and placed at different depths (Figure 2). The sensors were wrapped with geotechnical fabric to prevent direct contact between the sensors and the aquifer sand. Then the 5″ casing tubes were carefully taken out of the borehole, allowing the natural aquifer sand to fill the hole and leaving the sensors buried in the aquifer. Electric cables were connected from the sensors to a data logger at ground level, to enable collecting and recording the data from the sensors.

Field Measurements and Monitoring

After equilibration of the groundwater within the boreholes (a month after the end of drilling), EC profiles were made in the long-perforated boreholes, and a cross section of the transition zone perpendicular to shoreline was constructed (Figure 3). Sensors of water level, barometric pressure and EC were lowered into the boreholes for monitoring these parameters. Four EC sensors and a water level sensor were lowered into LP-3 to the same depths as the buried sensors in B-1, and two EC sensors were lowered into the short-perforated zones of SP-1 and SP-2 (Figure 2). All sensors (including the buried ones) were calibrated prior to their installation in the field. The sensors measured EC, temperature, water pressure, and barometric pressure every 15 min for 3 months between May and August 2011. All EC measurements were normalized to 25°C by the equation: $EC_{(25°C)} = EC_{(measured)}/(1 + 0.02\cdot(T_{(measured)} - 25))$ (McPherson 1997).

Another method of examining the short-term changes of the transition zone as affected by tidal fluctuations was done by using four EC profiles which were made in borehole LP-3 at different stages of the semidiurnal tide cycle. Stage I was high-tide, stage II was mid-tide on the ebb, stage III was low-tide, and stage IV was mid-tide at sea rising. These profiles were taken on August 28, which was in the spring tide period. Sea level data from Ashqelon, 10 km south of the research area, was obtained by the Survey of Israel (SOI).

Results

Groundwater Level

Groundwater level fluctuations in the boreholes adjacent to the sea, which were caused by the sea tide, decrease as distance from the shoreline increases. The amplitude of groundwater fluctuations in the LP-3 borehole (70 m from the shoreline) was around 2 cm at neap tide and around 7 cm at spring tide (Figure 4A), while in LP-1 (20 m from the shoreline) it was 6 to 20 cm, respectively. Even though the measurements were taken in the dry season (May to August), when there is no recharge to the aquifer, mean groundwater level increased about 20 cm during that period (Figure 4A). In addition to the general rising of the groundwater level, there were five events in which significant and sharp rises were monitored. The groundwater level rose sharply by around 10 cm and after several hours reverted back to a normal level.

EC Profiles

Results of four EC profiles, taken in the LP-3 borehole at different stages of the semidiurnal tide cycle, are presented in Figure 5A. EC values of high-tide profile are the highest at all depths and those of low-tide are the lowest. At both mid-tide profiles the EC values are in the middle between the high- and low-tide profiles. For discussion, these profiles were divided into three parts: (1) 0 to 5 mS/cm, (2) 5 to 32 mS/cm, and (3) 32 to 52 mS/cm.

While sea tide fluctuations are around 40 cm and groundwater fluctuations are around 7 cm (Figure 4A), those of the transition zone are 0.5 to 4 m between high- and low-tide EC profiles (Figure 5). In first and third parts of the profile (0 to 5 and 32 to 52 mS/cm, respectively) depth differences are much larger than in the second part of the profile (5 to 32 mS/cm). When observing the EC amplitude at specific levels, the largest amplitude was found around level -14.8 m above sea level (ASL), which is the location of EC sensor No. 2 (Figure 5B).

Groundwater level fluctuations in borehole LP-3 (located at distance of 70 m from the shoreline) have a time lag of about 3 h compared to the transition zone fluctuations. Thus, the highest groundwater level was measured 3 h after sea high tide, at mid tide on ebb, and the lowest groundwater level was measured three hours after sea low tide, at mid tide at sea rising (Figure 5C).

EC Fluctuations

The successive measurements of sea level, groundwater level, and EC in boreholes LP-3, SP-1, SP-2, and B-1, all located 70 m from shoreline, are presented in Figure 4. EC fluctuations in LP-3 are in the same periodicity as the sea tide in both daily and monthly tidal cycles. In neap tide periods EC fluctuations are relatively small, while in spring tide periods they are much larger. Since the upper EC sensor (pink line in Figure 4B) is located on the upper part of the transition zone between the fresh and saline water, it measures fresh water (<1 mS/cm) and shows almost no fluctuations at neap tide. At spring tide, when fluctuations are much more significant, the EC value rises up to 5 mS/cm. The second EC sensor (blue line) shows the most significant fluctuations. EC values vary between nearly fresh water (~1 mS/cm) to those of brackish water (~20 mS/cm), with an average EC value of around 15 mS/cm. The third EC sensor (green line) has smaller fluctuations than the second one, EC values vary between 22 and 32 mS/cm and its average value is around 28 mS/cm. The deepest sensor (orange line)

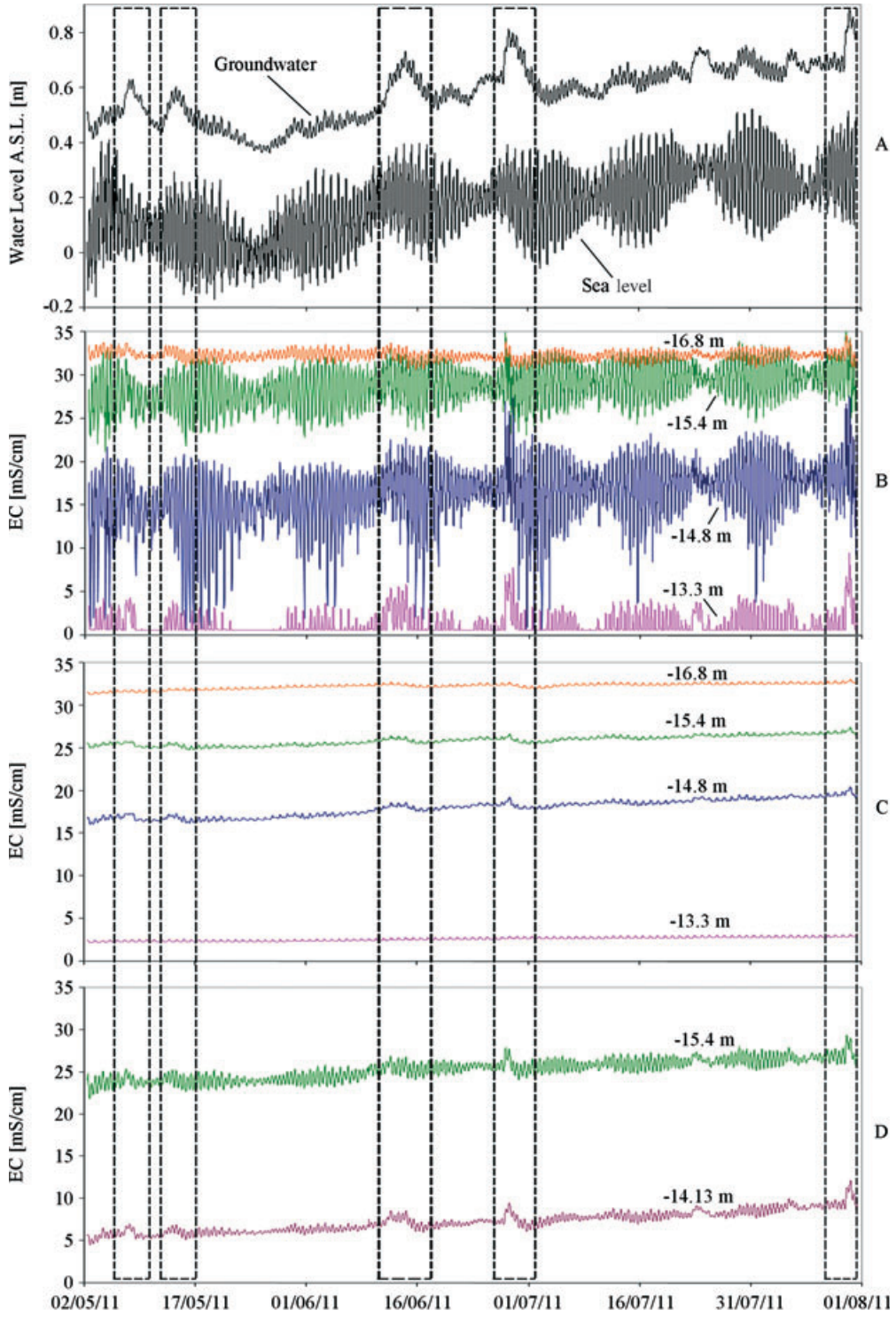

Figure 4. Top to bottom: (A) Sea level and groundwater level in LP-3; (B) EC in four sensors located at different depths in long-perforated borehole LP-3; (C) EC in four sensors buried at the same depths in B-1; and (D) EC in two sensors located at different depths in short-perforated boreholes SP-1 and SP-2. The broken frames represent events with a sharp rise in groundwater level due to stormy sea. Numbers on B, C, and D represent the depths of the sensors.

has relatively small fluctuations and its average EC value is around 32 mS/cm.

However, in the buried sensors, in B-1 (Figure 4C), the picture is completely different. EC values are quite stable and the amplitudes of the EC fluctuations in all four buried sensors are significantly smaller than in the long-perforated LP-3 borehole (~0.5 mS/cm). The oscillations of the transition zone due to tide in the aquifer itself seems to be on the scale of few centimeters. Yet, the effect of the daily sea tide is clearly detected in both neap and spring periods. In the short-perforated boreholes (SP-1 and SP-2; Figure 4D), the amplitude is somewhat larger (~1 to 2 mS/cm) compared to the buried sensors, but much smaller than in the long-perforated borehole.

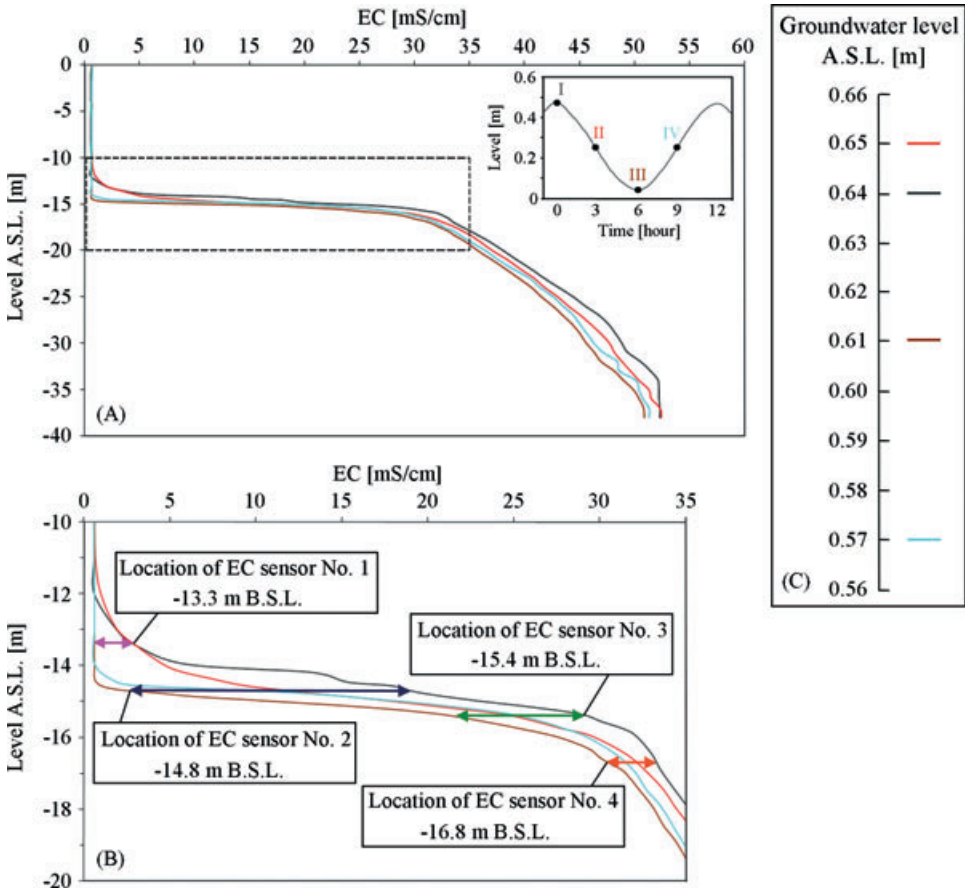

Figure 5. EC profiles and groundwater level in borehole LP-3 (long-perforated) on four stages of daily tide cycle on 28/8: I – High tide; II – Mid-tide on ebb; III – Low tide; and IV – Mid tide at sea rise. Zoom-in of the broken frame is presented in the lower part of the figure.

During 3 months of measurements, five events of significant and sharp rising of the groundwater level were measured in LP-3 (Figure 4A). Noticeable is that EC values in most sensors have also increased during the same periods. The most significant changes are seen on the EC sensors within the long-perforated borehole (LP-3), but small changes are seen also on the EC sensors within the short-perforated boreholes and on the buried sensors.

Discussion

The differences obtained between the EC sensors within the long-perforated borehole, the buried sensors, and those within the short-perforated boreholes, allow a better understanding of the main processes that affect monitoring of the transition zone between fresh and saline waters in coastal aquifers. The specific differences and their consequences are discussed in the following paragraphs.

Long-Perforation Bias

EC Profiles

EC profiles which were measured in the different stages of the semidiurnal tide (Figure 5), demonstrate the influence of long-perforation and sea tide on monitoring of the transition zone in coastal aquifers. The transition zone within the long-perforated borehole is strongly affected by tidal fluctuations and moves up and down every 6 h, at the same frequency as the semidiurnal tidal cycle. The EC profiles of two mid-tide measurements are in-between the profiles of high and low-tide measurements. Nevertheless, on an EC range of 0 to 5 mS/cm the profile of mid-tide on ebb is quite similar to the profile of high-tide, while the profile of mid-tide at sea rising is quite similar to the low-tide profile. These results could indicate the existence of hysteresis in the hydraulic system of the transition zone. It seems that the system has a "memory" and each step of the process depends on the previous step.

The vertical movement of the transition zone in the long-perforated borehole within a period of 6 h is some orders of magnitude larger than the real movement, which seems to be on the scale of a few centimeters (Shalev et al. 2009), considering sea tidal and groundwater fluctuations. Monitoring the transition zone in such boreholes might be unreliable since it moves up and down every 6 h and the differences are significant.

Successive Data

The successive data from the sensors within the LP-3, B-1, SP-1, and SP-2 boreholes (Figure 4) complement the results of the EC profiles. The significant differences in the EC fluctuations between the sensors in the long-perforated borehole and the buried sensors are due to a vertical flow

which occurs in the long-perforated boreholes, since it acts as "short circuits" along the vertical gradient as explained and simulated by Shalev et al. (2009).

At high tides, the hydraulic head of the sea water increases and the hydraulic gradient in the shoreline vicinity causes landward flow, so saline water intrudes into the aquifer. As a result, saline water in the lower part of the borehole has a higher hydraulic head than that of the fresh water in the upper part of the borehole. This hydraulic gradient induces upward flow within the borehole. At low tides, the reverse process happens, namely, the hydraulic head of sea water decreases and the hydraulic gradient inverses so both fresh and saline water flow seaward. In this case, the hydraulic head of fresh water in the upper part of the borehole is higher than that of the saline water, so downward flow occurs in the borehole. Such vertical flows occur in the borehole since its effective conductivity is many orders of magnitude higher than the hydraulic conductivity of the aquifer and therefore it acts as "short circuits." However, in the aquifer such vertical flows do not occur, since the whole process is diminished by the porous medium.

In the short-perforated boreholes some vertical flow does occur, but it seems that the short-perforation diminishes most of the vertical flow within the borehole and the EC fluctuations are much smaller than in the long-perforated boreholes. Thus, more accurate and reliable monitoring of the transition zone is achieved.

EC amplitudes of the sensors within LP-3 (Figure 4) are in good agreement with the EC amplitudes measured at the same depths between the EC profile of high- and low-tide (Figure 5B). Direct measurements of the aquifer, using the buried sensors, demonstrate that all the significant changes measured in the long-perforated borehole adjacent to the sea are in fact biased results caused by the long-perforation. Thus, the method of buried EC sensors is the best possible method for obtaining the true data from the aquifer itself.

Water Level Changes

Mean groundwater level increased by about 20 cm from May to August, even though it was a dry season with almost no precipitation. The sea water level in the same period shows the same trend (Figure 4A). The increase of mean sea level during the summer in the eastern Mediterranean Sea results from two main reasons (Striem and Rosenan 1972): (1) a decrease of barometric pressure during the summer and (2) the thermal expansion of sea water caused by the increasing temperature of the epilimnion by around 10 °C. Thus, it seems that the groundwater level in the vicinity of the sea is influenced by these changes rather than by terrestrial seasonal changes.

The events in which a sharp increase in groundwater level was measured are probably a consequence of stormy weather with high waves in the sea. This is supported by both field observation of waves (on two of the events of such sharp increase) and by measurements in the LP-1 and LP-2 boreholes. Inversion of the hydraulic gradient in the aquifer adjacent to the sea which was measured during these events caused groundwater flow from the sea to the aquifer. This is also the reason for the increase in EC values in the boreholes adjacent to the sea. Once again, the long-perforated borehole is much more affected than the buried sensors or the short-perforated boreholes. The mechanism which causes the rise of groundwater level and EC is quite similar to the tide effect on groundwater. In stormy weather with high waves, the hydraulic head of sea water increases and then sea water flows landward into the aquifer (Cartwright et al. 2004).

Both seasonal and daily changes in the groundwater level demonstrate that in the vicinity of the sea the main factor which influences the groundwater system is sea level changes, rather than terrestrial ones.

Time Series Analysis—Fast Fourier Transform Analysis

To determine the frequencies at which the fluctuations of groundwater level and the transition zone occur, and to estimate the driving force of these fluctuations, data-series of sea level, groundwater level in LP-3 (long-perforated borehole), EC in LP-3, and EC in B-1 (buried sensors) were analyzed by Fast-Fourier-Transform (FFT) analysis. The results were compared to the major tidal constituents typical for mixed tide.

Main frequencies and periodicities obtained by FFT analysis are presented in Table 2. The fluctuations of sea level, which are assumed to be the driving force of groundwater level and transition zone fluctuations, were found to be composed of all five tidal constituents, as expected (Figure 6A).

FFT analysis in the LP-3 time-series (water level and EC sensors) gives a very similar picture to that of the sea level: the fluctuations were composed of all five tidal constituents (except constituent N_2 in the LP-3 water level series), and the most dominant tidal constituent is the lunar semidiurnal (M_2), which is the major component of mixed tide (Table 2; Figure 6B and 6C). This similarity demonstrates that the groundwater level and the transition zone within long-perforated boreholes are strongly affected by sea tide. Tidal influence is also evident in the FFT results of the buried sensors, but less significantly. Only two tidal constituents (S_2 and K_2) were detected in all four buried sensors, and another (M_2) was found in two of the sensors (Table 2; Figure 6D).

It should be noted that the FFT results in the low frequencies (0 to 0.5 d-1) include a lot of noise, probably because the duration of measurements (around 3.5 months), was not long enough for detecting such frequencies. FFT analysis of a longer period of measurement should decrease this noise, and will probably include the periodicity of 14.75 d, which is the period between neap and spring tides.

From the results of the FFT analysis, it is clear that the sea tide is the driving force for the fluctuations of groundwater level and the transition zone within the LP-3 borehole. Most of the periodicities which compose the tide phenomenon in the sea also compose the fluctuations of groundwater level and EC in this borehole. The sea tide also influences the aquifer itself, as evidenced by the buried sensors analysis, but once again, as evident from the successive data (Figure 4), the influence in the aquifer is much smaller than in the long-perforated borehole. Further measurements and time series analyses are required in order to

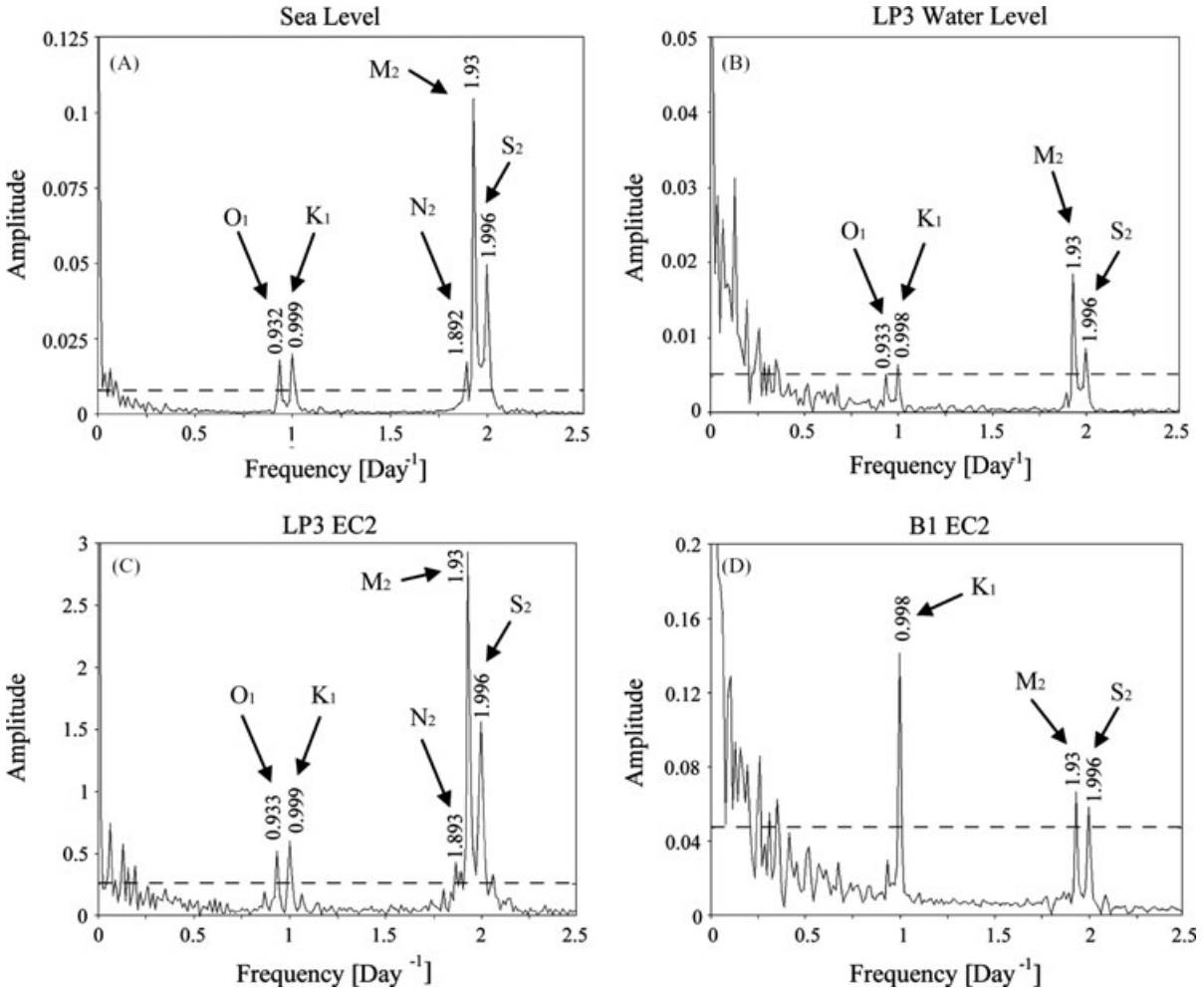

Figure 6. Main frequencies of sea level, groundwater level and sensor EC2 from the LP-3 borehole (long-perforated) and sensor EC2 from the buried sensor in B1, as obtained by Fast-Fourier-Transform (FFT) analysis. The broken line represents a significance of 95%. Low frequencies (0 to 0.5 d^{-1}) include a lot of noise due to the relatively short duration of measurement. Note that the amplitude axes on the different graphs are not on the same scale.

get a better understanding of the interaction between sea water and groundwater, and the dynamics between these two water bodies, but that is beyond the scope of this discussion.

Summary and Conclusions

Field data from the Israeli coastal aquifer validates the numerical model suggested by Shalev et al. (2009), showing that the significant fluctuations of the transition zone between fresh and saline water, which were measured in long-perforated boreholes in the vicinity of the shoreline, are a consequence of distortion caused by the flow regime within the boreholes. Thus, these fluctuations do not represent the actual behavior of the transition zone in the aquifer. The transition zone within the long-perforated boreholes is significantly affected by tidal oscillations, which cause vertical flow within the borehole that does not exist in the aquifer.

Measurements within short-perforated boreholes show that this kind of borehole diminishes the distortion dramatically. Even though EC fluctuations were larger than in the aquifer itself, the short-perforation reduced most of the vertical flow, and thus EC fluctuations were much smaller than in the long-perforated borehole. Therefore, short-perforation measurements should be considered to be more reliable and representative monitoring of the aquifer.

The most accurate method is the direct measurements through the buried sensors. These measurements show that the real EC fluctuations in the aquifer are much smaller than the EC fluctuations in the long-perforated borehole (a few centimeters compared to several meters). Thus, buried sensors are probably much more accurate for monitoring the real fluctuation of the transition zone.

FFT analysis shows that sea tidal oscillations are the driving force of groundwater level and transition zone EC fluctuations measured in long-perforated boreholes adjacent to the shoreline. The aquifer itself also seems to be influenced by the sea tide as evidenced by the periodicities in the buried sensors.

Considering all the above, we believe that the present monitoring of the transition zone in the vicinity of the shoreline through long-perforated boreholes is unreliable, since

Table 2

Main Frequencies and Periodicities of Sea Level, Groundwater Level and EC from LP-3 Borehole and EC from the Buried Sensors at B1, as Obtained by Fast-Fourier-Transform Analysis

	Tidal Constituent	Lunar Declinational Diurnal	Luni-Solar Declinational Diurnal	Larger Lunar Elliptic Semidiurnal	Lunar Semidiurnal	Solar Semidiurnal
Symbol		O_1	K_1	N_2	M_2	S_2
Sea Level	Frequency (solar day^{-1})	0.932	0.999	1.892	1.930	1.996
	Periodicity (solar day)	1.073	1.001	0.529	0.518	0.501
	Amplitude	0.018	0.020	0.017	0.105	0.050
LP3 Water level	Frequency (solar day^{-1})	0.933	0.998		1.930	1.996
	Periodicity (solar day)	1.072	1.002		0.518	0.501
	Amplitude	0.005	0.006		0.019	0.009
LP3 EC1	Frequency (solar day^{-1})	0.932	0.998	1.882	1.930	1.995
	Periodicity (solar day)	1.073	1.002	0.531	0.518	0.501
	Amplitude	0.240	0.251	0.143	0.781	0.414
LP3 EC2	Frequency (solar day^{-1})	0.933	0.999	1.893	1.930	1.996
	Periodicity (solar day)	1.072	1.001	0.528	0.518	0.501
	Amplitude	0.524	0.609	0.368	2.937	1.572
LP3 EC3	Frequency (solar day^{-1})	0.933	0.999	1.892	1.930	1.996
	Periodicity (solar day)	1.072	1.001	0.529	0.518	0.501
	Amplitude	0.249	0.332	0.298	2.083	0.985
LP3 EC4	Frequency (solar day^{-1})	0.933	0.999	1.893	1.930	1.996
	Periodicity (solar day)	1.072	1.001	0.528	0.518	0.501
	Amplitude	0.090	0.099	0.067	0.491	0.244
B1 EC1	Frequency (solar day^{-1})		0.998			1.996
	Periodicity (solar day)		1.002			0.501
	Amplitude		0.115			0.042
B1 EC2	Frequency (solar day^{-1})		0.998		1.930	1.996
	Periodicity (solar day)		1.002		0.518	0.501
	Amplitude		0.141		0.067	0.059
B1 EC3	Frequency (solar day^{-1})		0.998		1.930	1.996
	Periodicity (solar day)		1.002		0.518	0.501
	Amplitude		0.130		0.036	0.049
B1 EC4	Frequency (solar day^{-1})		0.998			1.996
	Periodicity (solar day)		1.002			0.501
	Amplitude		0.119			0.042

the location and shape of the transition zone change consistently every 6 h, correspondingly to sea tide variations. Thus, we suggest two alternative methods, short-perforation and buried sensors, for monitoring the transition zone more accurately.

Acknowledgment

This study was financed by the Israeli Water Authority and USAID—Middle East Regional Cooperation (MERC) Program. We thank H. Hemo (GSI) for all field work and general help. We thank Y. Meltzer and H. Srebro (SOI) for supplying sea level data.

References

Ataie-Ashtiani, B., R.E. Volker, and D.A. Lockington. 1999. Tidal effects on sea water intrusion in unconfined aquifers. *Journal of Hydrology* 216, no. 1–2: 17–31.

Bear, J. 1972. *Dynamics of Fluids in Porous Media*. ed. A.K. Biswas. New York: American Elsevier.

Bear, J. 1979. *Hydraulics of groundwater*. New York: McGraw-Hill Publishing Company.

Boon, J.D. 2004. *Secrets of the Tide - Tide and Tidal Current Analysis and Predictions, Storm Surges and Sea Level Trends*. Chichester, UK: Horwood Publishing.

Cartwright, N., L. Li, and P. Nielsen. 2004. Response of the salt-freshwater interface in a coastal aquifer to a wave-induced

groundwater pulse: Field observations and modelling. *Advances in Water Resources* 27 , no. 3: 297–303.

Church, P.E., and G.E. Granato. 1996. Bias in ground-water data caused by well-bore flow in long-screen wells. *Ground Water* 34, no. 2: 262–273.

Cooper, H.H. 1959. A hypothesis concerning the dynamic balance of fresh water and salt water in a coastal aquifer. *Journal of Geophysical Research* 64: 461–467.

Elci, B.A., F.J. Molz, 3rd, and W.R. Waldrop. 2001. Implications of observed and simulated ambient flow in monitoring wells. *Ground Water* 39, no. 6: 853–862.

Issar, I. 1968. Geology of the central coastal plain of Israel. *Israel Journal of Earth Sciences* 17: 16–29.

Kim, J.H., J. Lee, T.J. Cheong, R.H. Kim, D.C. Koh, J.S. Ryu, and H.W. Chang. 2005. Use of time series analysis for the identification of tidal effect on groundwater in the coastal area of Kimje, Korea. *Journal of Hydrology* 300, no. 1–4: 188–198.

Kim, K.Y., H. Seong, T. Kim, K.H. Park, N.C. Woo, Y.S. Park, G.W. Koh, and W.B. Park. 2006. Tidal effects on variations of fresh-saltwater interface and groundwater flow in a multilayered coastal aquifer on a volcanic island (Jeju Island, Korea). *Journal of Hydrology* 330, no. 3–4: 525–542.

Kohout, F. 1960. Cyclic flow of salt water in the Biscayne aquifer of southeastern Florida. *Journal of Geophysical Research* 65: 2133–2141.

Konikow, L.F., and G.Z. Hornberger. 2006. Modeling effects of multimode wells on solute transport. *Ground Water* 44, no. 5: 648–660.

Lutzki, H., and E. Shalev. 2010. Slug test for measurements of hydraulic conductivity and boreholes intactness at the coastal plain aquifer: Geological Survey of Israel Report (in Hebrew).

McPherson, L.L. 1997. Using correct conductivity temperature compensation. *Water-Engineering & Management* 144, no. 5: 36.

Melloul, A.J. 1988. Atlas of Israel coastal plain aquifer geometry and physical properties: Israel Hydrological Service (in Hebrew).

Melloul, A.J., and D.G. Zeitoun. 1999. A semi-empirical approach to intrusion monitoring in Israeli coastal aquifer. In *Seawater Intrusion in Coastal Aquifers - Concepts, Methods and practices*, ed. J. Bear. Dordrecht, The Netherlands: Kluwer Academic Publishers.

Nativ, R., and N. Weisbrod. 1994. Hydraulic connections among sub-aquifers of the Coastal Plain Aquifer. *Israel Ground Water* 32, no. 6: 997–1007.

Nielsen, P. 1990. Tidal dynamics at water table in beaches. *Water Resources Research* 26: 2127–2134.

Pugh, D.T. 1996. *Tides, Purges and Mean Sea Level*. Chichester, UK: John Wiley & Sons Ltd.

Robbins, G.A. 1989. Influence of using purged and partially penetrating monitoring wells on contaminant detection, mapping, and modeling. *Ground Water* 27, no. 2: 155–162.

Shalev, E., A. Lazar, S. Wollman, S. Kington, Y. Yechieli, and H. Gvirtzman. 2009. Biased monitoring of fresh water-salt water mixing zone in coastal aquifers. *Ground Water* 47, no. 1: 49–56.

Strack, O.D.L. 1976. A single-potential solution for regional interface problems in coastal aquifers. *Water Resources Research* 12, no. 6: 1165–1174.

Striem, H.L., and N. Rosenan. 1972. Seasonal fluctuations of monthly mean sea-level on coast of eastern mediterranean. *International Hydrographic Review* 49, no. 2: 129.

Todd, D.K. 1980. *Ground-Water Hydrology,* 2nd ed. New York: John Wiley and Sons.

Underwood, M.R., F.L. Peterson, and C.I. Voss. 1992. Groundwater lens dynamics of atoll islands. *Water Resources Research* 28, no. 11: 2889–2902.

Van Dam, J.C. 1999. Exploitation restoration and management: In *Seawater Intrusion in Coastal Aquifers – Concepts, Methods and Practices*, ed. J. Bear. Dordrecht, The Netherlands: Kluwer Academic Publishers.

Wang, J., and T.K. Tsay. 2001. Tidal effects on groundwater motions. *Transport in Porous Media* 43, no. 1: 159–178.

Yechieli, Y., and A. Hadad. 2009. Hydrogeological findings from new boreholes for monitoring seawater intrusion, perpendicular to the shoreline at Ashdod site: Geological Survey of Israel.

Biographical Sketches

E. Levanon, *corresponding author, is with the Institute of Earth Sciences, Hebrew University of Jerusalem and Geological Survey of Israel (GSI), Jerusalem, Israel; eladlevanon@gmail.com*

Y. Yechieli *is with the Geological Survey of Israel (GSI), Jerusalem, Israel.*

E. Shalev *is with the Geological Survey of Israel (GSI), Jerusalem, Israel.*

V. Friedman *is with the Hydrological Service, Israel Water Authority, Jerusalem, Israel.*

H. Gvirtzman *is with the Institute of Earth Sciences, Hebrew University of Jerusalem, Jerusalem, Israel.*